Real-Time Imaging of Nuclear Permeation by EGFP in Single Intact Cells

Xunbin Wei, Vanessa G. Henke, Carsten Strübing, Edward B. Brown,* and David E. Clapham
Howard Hughes Medical Institute, Children's Hospital, *E.L. Steele Laboratory, Department of Radiation Oncology, Massachusetts General Hospital, Harvard Medical School, Boston, Massachusetts 02115

ABSTRACT The NPC is the portal for the exchange of proteins, mRNA, and ions between nucleus and cytoplasm. Many small molecules (<10 kDa) permeate the nucleus by simple diffusion through the pore, but molecules larger than 70 kDa require ATP and a nuclear localization sequence for their transport. In isolated *Xenopus* oocyte nuclei, diffusion of intermediate-sized molecules appears to be regulated by the NPC, dependent upon [Ca^{2+}] in the nuclear envelope. We have applied real-time imaging and fluorescence recovery after photobleaching to examine the nuclear pore permeability of 27-kDa EGFP in single intact cells. We found that EGFP diffused bidirectionally via the NPC across the nuclear envelope. Although diffusion is slowed ~100-fold at the nuclear envelope boundary compared to diffusion within the nucleus or cytoplasm, this delay is expected for the reduced cross-sectional area of the NPCs. We found no evidence for significant nuclear pore gating or block of EGFP diffusion by depletion of perinuclear Ca^{2+} stores, as assayed by a nuclear cisterna-targeted Ca^{2+} indicator. We also found that EGFP exchange was not altered significantly during the cell cycle.

INTRODUCTION

The eukaryotic NPC spans the concentric bilayer of the NE to connect the cytoplasm and the nucleoplasm (Allen et al., 2000; Keminer and Peters, 1999). The lumen of the NE (nuclear cisterna or perinuclear space) is continuous with that of the endoplasmic reticulum and its outer membrane protein composition is similar to that of the rough endoplasmic reticulum. The inner membrane anchors chromatin on its nucleoplasmic face and components of the nuclear lamina on its perinuclear face (Ellenberg et al., 1997; Foisner and Gerace, 1993). The NPC, a supramolecular protein complex of 124,000 kDa, controls nucleo-cytoplasmic exchange of protein and mRNA, necessary for cell growth and responses to extracellular signals (Keminer and Peters, 1999; Wang and Clapham, 1999; Wente, 2000). Most ions and proteins of molecular weight <~10 kDa cross the NPC by passive diffusion (Perez-Terzic et al., 1996), whereas macromolecules >~70 kDa require an NLS and energy-dependent processes to traverse the NPC (Hicks and Raikhel, 1995). Active transport was reported to be blocked under similar conditions (Greber and Gerace, 1995), but Strübing et al. recently demonstrated that active nuclear import and export was independent of perinuclear Ca^{2+} stores in intact mammalian cells (Strubing and Clapham, 1999).

Stehno-Bittel et al. found that isolated *Xenopus* oocytes nuclei were impermeant to intermediate-sized (roughly 10–70 kDa) fluorescent molecules after Ca^{2+} store depletion conditions were imposed (Stehno-Bittel et al., 1995). Perez-Terzic et al. found that nuclear pores from isolated *Xenopus* oocytes nuclei undergo conformational changes by atomic force microscopy under these conditions (Perez-Terzic et al., 1996). Nuclear pore conformational changes have also been noted in isolated nuclei in two other laboratories using atomic force microscopy (Danker and Oberleithner, 2000; Shahin et al., 2001; Stoffler et al., 1999), and more recently again in our own laboratory (Wang and Clapham, 1999). In isolated nuclei there is thus strong evidence for nuclear pore conformational changes, but the mechanism is a matter of debate. Notably, these papers only report isolated nuclei, and the obvious question is whether other alterations occur when isolating the nuclei from their cytoplasmic environment. To address this issue in intact cells, Perez-Terzic et al. (1999) found that the cardiac nuclear pore in intact cells was also impermeant to intermediate-sized molecules under Ca^{2+} store depletion conditions. Here we examine the issue of permeation of 10, 27, 56, and 70 kDa proteins via the NPC under Ca^{2+} store depletion conditions by a variety of methods and throughout the cell cycle. For 10, 27, and 56 kDa proteins, diffusion is slowed ~100-fold at the NE boundary compared to diffusion within the nucleo- or cytoplasm, as expected for the reduced cross-sectional area of the NPCs. We found no evidence for significant nuclear pore gating or block of EGFP diffusion despite depletion of perinuclear Ca^{2+} stores by multiple methods. EGFP, a non-native 27-kDa fluorescent protein, does not contain a nuclear localization sequence. Photobleaching has often been used to reveal the dynamics of free and protein bound fluorophores (White and Stelzer, 1999). The process of photobleaching

Submitted July 5, 2002, and accepted for publication October 17, 2002.

Address reprint requests to Dr. David E. Clapham, Rm. 1309, Enders Bldg., P.O. Box EN-306, Children's Hospital, 320 Longwood Ave., Boston, MA 02115. Tel.: 617-355-6163; Fax: 617-731-0787; E-mail: dclapham@enders.tch.harvard.edu.

Abbreviations used: NPC, nuclear pore complex; CFP, cyan fluorescence protein; DOG, 2-deoxyglucose; FCCP, carbonyl cyanide p-trifluoromethyloxyphenylhydrazone; EGFP, enhanced green fluorescence protein; FRAP, fluorescence recovery after photobleaching; FRET, fluorescence resonance energy transfer; LBR, lamin B receptor; NE, nuclear envelope; NLS, nuclear localization sequence; TPEN, tetrakis-[2-pyridylmethyl]-ethylenediamine; YC, yellow cameleon; YFP, yellow fluorescence protein.

© 2003 by the Biophysical Society

0006-3495/03/02/1317/11 $2.00

results in an irreversible photochemical change in the fluorophore structure so that it no longer fluoresces (Rost, 1992; Tsien and Waggoner, 1995). Thus, recovery does not refer to the return of bleached fluorophores to light-emitting configurations, but rather the diffusion of unbleached fluorophores into volumes containing photobleached (dark) molecules. When EGFP in the whole nucleus or the cytoplasm is photobleached, FRAP can be used to monitor the movement of the molecule between the two cell compartments. Previous FRAP studies of enhanced GFP indicated that EGFP readily diffuses within both the nuclear and cytoplasmic compartments (Patterson et al., 1997; Seksek et al., 1997; Swaminathan et al., 1997; Tsien, 1998; Wachsmuth et al., 2000; Yokoe and Meyer, 1996).

MATERIALS AND METHODS

Cell culture and transfection

COS7 cells were grown in Dulbecco's modified Eagle's medium (DMEM) supplemented with 10% fetal calf serum and maintained in a humidified incubator at 37°C (5% CO_2). HEK 293 cells were grown at 37°C (5% CO_2) in DMEM/F12 (1:1) medium supplemented with 10% fetal calf serum, 2 mM glutamine, 100 U/ml penicillin, 100 μg/ml streptomycin, and HT supplement (1:100; Gibco-BRL, Gaithersburg, MD). HM-1 cells, from a human embryonic kidney cell line stably expressing the muscarinic M1 receptor, were grown at 37°C (5% CO_2) in DMEM/F12 (1:1) medium supplemented with 10% fetal calf serum, 2 mM glutamine, 100 U/ml penicillin, 100 μg/ml streptomycin, 0.5 mg/ml G418, and HT supplement (1:100; Gibco-BRL). Primary neonatal cardiomyocytes were prepared from 2- to 3-day-old rats (Harlan Sprague-Dawley, Cambridge, MA) after ventricles were separated and cut into 1-mm^3 pieces. Tissue was digested (overnight, 4°C) in 10 ml Hanks' buffer with 10 mM HEPES, 8 mM $MgCl_2$, and 500 μg trypsin (Worthington Biochemicals, Lakewood, NJ). The cell mixture was then treated with 200 μg/ml trypsin inhibitor and 90 U/ml collagenase (Worthington Biochemicals) and incubated at 37°C for 20 min. Cells were centrifuged at 1000 rpm for 5 min. The pellet was suspended in plating medium, DMEM (Gibco-BRL) with 10% fetal bovine serum and penicillin/streptomycin (50 U/ml, Gibco-BRL). Cells were plated on coverslips (37°C, 5% CO_2). Cells were transfected with pEGFP-N1 vector (Clontech Laboratories, Palo Alto, CA) using lipofectamine 2000 reagent (Life Technologies, Gaithersburg, MD; according to the manufacturer's instructions) ~24 h after plating onto 25-mm diameter coverslips. To confirm the depletion of perinuclear Ca^{2+} stores, cells were transfected with pcDNA3.1 vector containing LBR-YC (generously provided by Dr. Michael Badminton, University of Wales).

Construction of adenovirus and infection of COS7 cell

EGFP adenovirus Ad-EGFP was made by homologous recombination (He et al., 1998). The vectors pADTrack-CMV (kan) and pAdEasy-1 (Amp) were gifts from Dr. Bert Vogelstein (Johns Hopkins University). The electro-competent BJ5183 cells were used to achieve the highest frequency of homologous recombination. 100 ng pADTrack-CMV linearized by *Pme*I was cotransformed with 100 ng of pAdEasy-1 into BJ5183 cells. Recombinants were selected in L-broth plates containing 50 μg/ml of kanamycin and confirmed by restriction analysis with *Pac*I, *Spe*I, and *Bam*HI. 4 μg pAD-EGFP was then digested with *Pac*I and transfected in 2×10^6 HEK 293 cells in a 25-cm^2 flask using lipofectamine 2000 reagent. HEK 293 cells were harvested after 10 days. The medium was discarded and the cells were resuspended in 1 ml phosphate buffered solution. The virus was released by three freeze-thaw cycles and the virus titer was measured by plaque assay. COS7 cells were infected with Ad-EGFP at 100 multiplicity of infection for 48 h before FRAP measurement of nuclear permeation of EGFP.

Fluorescence imaging and photobleaching

Confocal imaging of EGFP was performed with a laser-scanning microscope (LSM 410, Carl Zeiss; 63× objective; 488-nm excitation; emission 510–545 nm). The pinhole size was set to 10, corresponding to an ~1 μm confocal slice. For FRAP analysis, a 72 × 72 pixel area within the nucleus or the cytoplasm was photobleached for 8 s (~0.3 mW). After photobleaching, the microscope was immediately switched to imaging mode (~0.003 mW). Time-lapse sequences were recorded every 2 s for 10 min. The background was subtracted from the images before analysis. All FRAP experiments were performed at 37°C as well as at room temperature (~22°C).

Depletion of perinuclear Ca^{2+} stores; FRET imaging by two-photon microscopy

Control COS7 cells were bathed in standard external solution, containing (in mM): 140 NaCl, 5.4 KCl, 2 $CaCl_2$, 1 $MgCl_2$, and 10 HEPES adjusted to pH 7.4 (22°C). To deplete intracellular Ca^{2+} stores (including perinuclear Ca^{2+} stores), cells were first washed three times in nominally Ca^{2+}-free solution containing (in mM): 140 NaCl, 5.4 KCl, 1 $MgCl_2$, 1 EGTA, and 10 HEPES adjusted to pH 7.4. Subsequently, cells were incubated at 37°C with 1, 3, or 20 μM ionomycin (Ca^{2+} ionophore) for 20 min, 3 μM thapsigargin (Ca^{2+}-ATPase inhibitor) for 90 min, 10 or 20 μM BAPTA-AM (Ca^{2+} chelator) for 30 min, 50 μM A23187 (Ca^{2+} ionophore) for 20 min, or 100 μM TPEN for 60 min, respectively. TPEN is a chelator with much higher affinity for heavy metal ions than BAPTA. These conditions completely emptied intracellular Ca^{2+} stores inasmuch as subsequent application of ionomycin (10 μM) in Ca^{2+}-free solution did not produce any further rise in the cytosolic Ca^{2+} concentration in Oregon-green/Fura-red-loaded cells (Molecular Probes, Eugene, OR). Perinuclear Ca^{2+} depletion was further monitored by FRET of LBR-YC transfected in COS7 cells (see Results). Cells were illuminated with a tunable, near infrared titanium: sapphire laser (820 nm) and the ratio of yellow (λ emission = 535 nm) to cyan (λ emission = 480 nm) was measured as a gauge of perinuclear Ca^{2+} concentration (Miyawaki et al., 1997). When perinuclear [Ca^{2+}] was depleted by various agents in a low [Ca^{2+}] buffer (estimated free [Ca^{2+}] = 10 nM), FRET declined (10–20%) to similar levels as observed by Miyawaki et al. (see Results).

Microinjections

HM-1 cells, MDCK cells, or primary neonatal cardiomyocytes were simultaneously microinjected with 2.5 mg/ml 10 kDa fluorescein-dextran and 70 kDa rhodamine-dextran in injection buffer. Cells were plated on coverslips 24–48 h before the experiments. Injections were performed using an Eppendorf 5242 microinjector (Eppendorf Scientific, Westbury, NY). The injection buffer contained 140 mM KCl, 1 mM EGTA, and 10 mM HEPES (pH 7.4). The injection volume was ~5–10% of the cell volume. Before microinjections, cells were preincubated for 30 min at 37°C in normal Ca^{2+} medium or in Ca^{2+}-free medium supplemented with 1.5 μM ionomycin or 1.5 μM thapsigargin. The normal Ca^{2+} medium contained DMEM/F12 (1:1) plus HT supplement and 1.5 mM $MgCl_2$. The Ca^{2+}-free medium contained F12 medium supplemented with HT, 2 mM EGTA, and 1.5 mM $MgCl_2$ (calculated free [Ca^{2+}] = 180 nM). Fluorescent dextrans were obtained from Molecular Probes (Eugene, OR). Cells were observed by confocal imaging 5–15 min after microinjection.

Cell synchronization and ATP/GTP depletion

COS7 cells were seeded at 10% density ~24 h before synchronization.

A population of cells reversibly synchronized at the G1/S boundary was obtained by supplying asynchronously growing cells for 20 h in DMEM/F12 supplemented with GHT (Gibco-BRL), 1% streptomycin/penicillin, 5% FCS, and 15 μM aphidicolin. Cells enriched in S phase (3.1×10^5 cells/ml) were obtained by removing aphidicolin from cells blocked at the G1/S boundary, rinsing three times with phosphate-buffered saline, and supplying them with fresh culture medium containing 10% FCS (Fatatis and Miller, 1999; Krek and DeCaprio, 1995; Liao et al., 1997). Based on prior studies, the cells reached the G2/M boundary ~10 h after release from aphidicolin (Krek and DeCaprio, 1995; Liao et al., 1997). Each cell was studied for 10 min by FRAP assay, and a total of 96 cells were sampled for a period of 24 h after release from aphidicolin block to ensure that the majority of cells completed at least one cell cycle. All FRAP experiments were carried out at 37°C as well as at room temperature. Cell proliferation was confirmed by cell counting (5.9×10^5 cells/ml). To obtain individual cells in the mitotic phase and during anaphase, the nuclear boundaries of cells in interphase were identified by YFP-LBR transfection labeling. Cells in interphase possessed a single morphologically recognizable nucleus. Such cells were followed individually to obtain cells at different stages in the cell cycle. The disappearance of the ring-like structure of the NE marked the mitotic phase of the cell. The cells in anaphase were identified by the presence of two newly formed nuclei. ATP/GTP depletion was achieved by the application of DOG (6 mM) and FCCP (1 μM) for 30 min at 37°C.

Quantitative analysis of nuclear EGFP FRAP due to transnuclear restricted diffusion

In EGFP-transfected cells, nuclear and cytoplasmic fluorescence intensities were obtained by LSM 410 software and analyzed using KaleidaGraph software. Traditional FRAP analysis deals with free diffusion, where the boundaries (barriers) of the system are effectively at infinity and do not influence the diffusive recovery kinetics. However, here we are dealing with restricted diffusion between two well-mixed compartments (the nucleus and the cytoplasm (see Fig. 1)) where the boundary properties (i.e., the permeability properties of the nuclear membrane due to a finite number of nuclear pores) strongly influence the diffusive recovery kinetics. Consequently, the post-bleach concentration dynamics of two connected well-mixed compartments is expected to be described by exponential decays (Majewska et al., 2000; Svoboda et al., 1996) as opposed to the infinite series solution of traditional FRAP analysis (Axelrod et al., 1976). If the nucleus is connected to the cytoplasm by a diffusive pathway of resistivity W (cm^{-1}), then the differential equations describing the post-bleach concentration dynamics of the nucleus and cytoplasm are:

$$\frac{\partial C_N(t)}{\partial t} = -\frac{D}{V_N W}\left(C_N(t) - C_C(t)\right) \tag{1}$$

$$\frac{\partial C_C(t)}{\partial t} = \frac{D}{V_C W}\left(C_N(t) - C_C(t)\right), \tag{2}$$

where $C_N(t)$ is the concentration of unbleached EGFP in the nucleus, $C_C(t)$ is the concentration of unbleached EGFP in the cytoplasm, V_N and V_C are the volume of the nucleus and cytoplasm, respectively, and D is the cytoplasmic diffusion coefficient of EGFP. W, the diffusive resistivity, is approximately equal to $L/(n_p\pi(R_P - R_{GFP})^2)$, where L is the mean length of the pores connecting the nucleus to the cytoplasm, n_p is the total number of accessible pores, R_P is the mean radius of the pore openings, and R_{GFP} is the hydrodynamic radius of EGFP. We make the approximation that the cytoplasmic volume is significantly larger than the nuclear volume. This

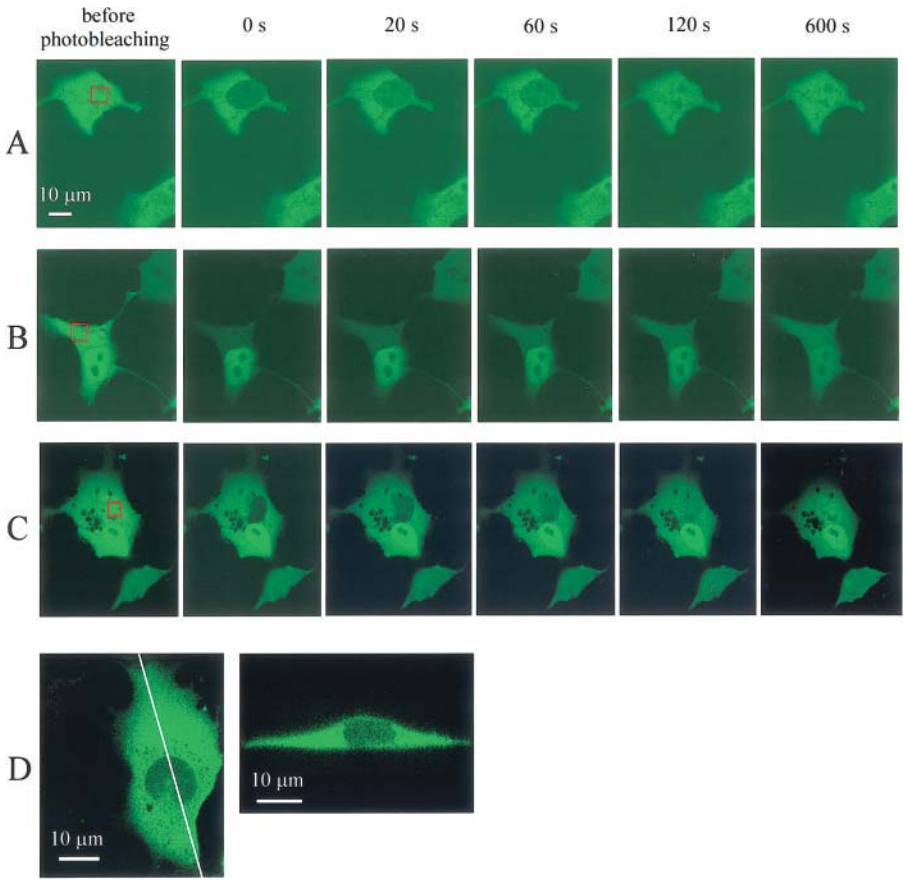

FIGURE 1 Nuclear permeation by EGFP. COS7 cells were transfected with EGFP (27 kDa) 24–48 h before imaging. An area (*red box*) within the nucleus or the cytoplasm of an $EGFP^+$ cell was photobleached using 488 nm light from an argon-krypton laser by single photon confocal scanning (0.3 mW at the nucleus for 8 s, or for 20 s at the cytoplasm). Fluorescence recovery in the photobleached compartment was then monitored at 20-s intervals for 10 min. (*A*) Fluorescence recovery after nuclear photobleaching as EGFP diffuses into the nucleus from the cytoplasm. Imaging acquisition necessitated an ~2 s delay after photobleaching. Therefore, equilibration within the nucleus was reached at $t = 0$ s (imaging acquisition time) when the square photobleached area had already recovered. (*B*) Cytoplasmic fluorescence recovery after cytoplasmic photobleaching as EGFP diffuses from the nucleus (nuclear fluorescence decreases). (*C*) Fluorescence recovery after nuclear photobleaching of one nucleus (*red box*) in a cell containing two nuclei. The second nucleus serves as an internal control. No significant bleaching occurred in the second nucleus as a result of laser scattering. (*D*) Two-dimensional reconstructed side view (*right*) of a COS7 cell after nuclear photobleaching of EGFP. The same cell in the *x-y* plane is shown at left. The white line denotes the location of the section used to construct the side view.

approximation allows us to gain insight into the physical parameters that affect the post-bleach recovery time of the nuclear EGFP fluorescence. We can therefore consider $C_C(t)$ as a constant (its change was relatively small in our experiments), and the solution to Eq. 1 becomes:

$$C_N(t) = C_C - \Delta C_N^0 e^{-t/\tau}, \quad (3)$$

where ΔC_N^0 is the initial decrease in nuclear EGFP concentration due to the bleaching pulse and τ is the diffusive recovery time, given by $\tau = LV_N/(D\, n_p\pi(R_P - R_{EGFP})^2)$. Over the time course of these experiments, the relationship between the concentration of EGFP in the nucleus and the fluorescence signal from the nucleus is expected to be constant. Therefore the fluorescence signal from the nucleus $F_N(t)$ is given by:

$$F_N(t) = F(\infty) - \Delta F_N^0 e^{-t/\tau}, \quad (4)$$

where $F(\infty)$ is the fluorescence signal at $t = \infty$ and ΔF_N^0 is the initial fluorescence change due to the bleaching pulse. Consequently, the exponential recovery time of the bleached nucleus is dependent upon the volume of the nucleus, the diffusion coefficient of EGFP, the number of accessible pores, and the pore channel geometry.

The permeability of the nuclear membrane, P, is defined as follows:

$$I = P(C_N - C_C)A_N, \quad (5)$$

where I is the current of EGFP exiting the nucleus, with units of s^{-1}, and A_N is the accessible area of the nuclear membrane. Comparison of Eqs. 1 and 5 and the definition of τ reveals that $P = V_N/A_N\tau$. If the nucleus is approximated as a sphere with a radius R_N, the permeability of the nuclear membrane is then given by:

$$P = \frac{R_N}{3\tau}. \quad (6)$$

For comparison with previous work on the diffusion of fluorescent molecules in the cells, we also fit the recovery of the nuclear EGFP signal with a conventional free-diffusion FRAP formula (Axelrod et al., 1976):

$$F(t) = F(\infty)\sum_{n=0}^{\infty}\frac{(-\beta)^n}{n!}\left(1 + n\left(1 + \frac{2t}{\tau_D}\right)\right)^{-1}, \quad (7)$$

where β is the bleach depth parameter, and τ_D is the diffusive recovery time. In the case of free diffusion, $\tau_D = \omega_r^2/4D$, where ω_r is the e^{-2} beam radius.

RESULTS

EGFP nuclear permeation measured by FRAP

We used FRAP to monitor the nuclear permeation of mammalian COS7 cells transfected with EGFP. The nucleus, or a segment of the cytoplasm, was photobleached and its subsequent fluorescence recovery due to movement of unbleached EGFP was recorded by confocal microscopy (Fig. 1). Fast equilibration of EGFP fluorescence within the nucleus or cytoplasm after photobleaching was always achieved within ~2 s. Our observations correlated well with previous FRAP studies showing that EGFP moves freely within these compartments (Patterson et al., 1997; Seksek et al., 1997; Swaminathan et al., 1997; Tsien, 1998; Wachsmuth et al., 2000; Yokoe and Meyer, 1996). To distinguish EGFP transnuclear movement from diffusion within the nucleus, a large photobleached area within the nucleus was used to ensure that the entire nucleus was photobleached (thus the recovery of fluorescence in the nucleus was a consequence of transport of EGFP from the cytoplasm). As EGFP diffused into the nucleus from the cytoplasm, there was a simultaneous decrease in cytoplasmic fluorescence. Similarly, after a large volume of the cytoplasm was photobleached (and thus the entire cytoplasm became uniformly darker due to free and fast diffusion of EGFP within the cytoplasm), fluorescence in the cytoplasm recovered coincident with a decrease in nuclear fluorescence (Fig. 1 *B*). Fluorescence recovery of either the nucleus or cytoplasm reached a plateau within 8–10 min with a half-life of ~2 min. The prolonged fluorescence recovery of either compartment compared to free diffusion is due to restricted diffusion across the nuclear envelope, consistent with the diffusion through the open NPCs (~0.01 of total NE surface area (see Discussion)). The fluorescence recovery experiments were performed at 37°C as well as at room temperature.

One initial concern in our experiments was that light might scatter outside the directly illuminated volume and bleach unintended areas. However, scattering was not significant over distances resolved by confocal microscopy (~300 nm in the x-y plane). For example, photobleaching of a volume of the bath solution did not photobleach a cell located 2 μm away (data not shown). In fact, when one nucleus was photobleached in a cell containing two nuclei, no significant bleaching occurred in the second immediately adjacent nucleus (Fig. 1 *C*).

A second concern was that because the continuous cytoplasmic volume was photobleached above and below the nucleus, this volume might add a significant component of unrestricted recovery. However, these volumes were small because the nucleus generally fills the space between the upper and lower plasma membranes in COS7 cells. Fast z-sectioning of the nucleus-photobleached cell demonstrated that the confocal images identified in the x-y plane indeed primarily represented either the nucleus or the cytoplasm (Fig. 1 *D*). Moreover, the nuclear fluorescence in each z plane confocal slice showed similar recovery rates (data not shown). Therefore, the fluorescence recovery was not due to EGFP diffusion within the same cell compartment from above or below the focal plane. Instead, the fluorescence recovery that we show here reflected primarily the diffusion of EGFP from the unbleached compartment, presumably through the NPCs.

A third concern was that laser illumination alone might damage membranes and produce holes in the nuclear membrane. The laser power used in our photobleaching experiments was ~0.3 mW and not likely to cause significant localized cell heating. Liu et al. (1995) have shown that 1064-nm wavelength laser illumination increased cell temperature by ~1.1°C/100 mW. The laser power used in our photobleaching experiments was ~0.3 mW (488 nm) and not likely to cause significant localized cell heating. In addition, two lines of evidence suggest that EGFP traffic is not a consequence of the photo damage to the NE. First, when a volume of the cytoplasm distant from the NE was

photobleached, fluorescence in the cytoplasm still recovered coincident with a decrease in nuclear fluorescence and there was no cytoplasmic fluorescence decrease due to leak through the cell membrane. Second, the molecular weight size restriction was preserved in laser-illuminated cells. In several previous studies, the molecular cut-off size for passive diffusion through the NPC was measured to be 60–70 kDa (Gerace and Burke, 1988; Schindler and Jiang, 1987). In agreement with this work, we observed nuclear FRAP of a 56 kDa EGFP-fusion protein (pcDIC35, provided by Anthony Persechini), but not a 70 kDa EGFP-fusion protein (pcDIC49; Romoser et al., 1997). The inability of 70 kDa EGFP-fusion protein to permeate the NE implies that the NE was not grossly damaged. Lastly, we varied the extent of photobleaching (two- to fourfold) and found that the recovery kinetics were not sensitive to the amount of illumination (data not shown), which indicated that bleaching was not generating some form of photodamage that could affect nuclear membrane permeability.

The kinetics of fluorescence recovery due to transnuclear restricted diffusion was measured after nuclear photobleaching. Before photobleaching, we recorded the fluorescence intensities in the nucleus and cytoplasm. A 72 × 72 pixel area within the nucleus was then photobleached for 8 s. The entire nucleus was photobleached and sequential confocal images of the entire cell were taken at 2-s intervals. Fluorescence intensity data from these images was used to measure nuclear fluorescence recovery as a function of time (Fig. 2 *A*; $n = 40$). Traditional FRAP analysis deals with free diffusion, where the boundaries (barriers) of the system are effectively at infinity and do not influence the diffusive recovery kinetics. However, here we are dealing with restricted diffusion between two well-mixed compartments (the nucleus and the cytoplasm (see Fig. 1)) where the boundary properties (i.e., the permeability properties of the nuclear membrane due to a finite number of nuclear pores) strongly influence the diffusive recovery kinetics. Consequently, the post-bleach concentration dynamics of two connected well-mixed compartments is expected to be described by exponential decays (Svoboda et al., 1996; Majewska et al., 2000; also see Materials and Methods) as opposed to the infinite series solution of traditional FRAP analysis (Axelrod et al., 1976). The fluorescence recovery of the nucleus was fit quite well with a simple exponential function (Fig. 2 *A*) and we compared the time constants of the best-fit single exponentials. The time constant (τ) of recovery of nuclear fluorescence was 164 ± 1.8 s (mean ± SE, $n = 40$). The permeability of the nuclear membrane P was estimated to be 0.011 μm/s (see Materials and Methods). The fluorescence in the cytoplasm decreased as EGFP diffused from the cytoplasm into the nucleus with a much smaller change in relative fluorescence, reflecting the

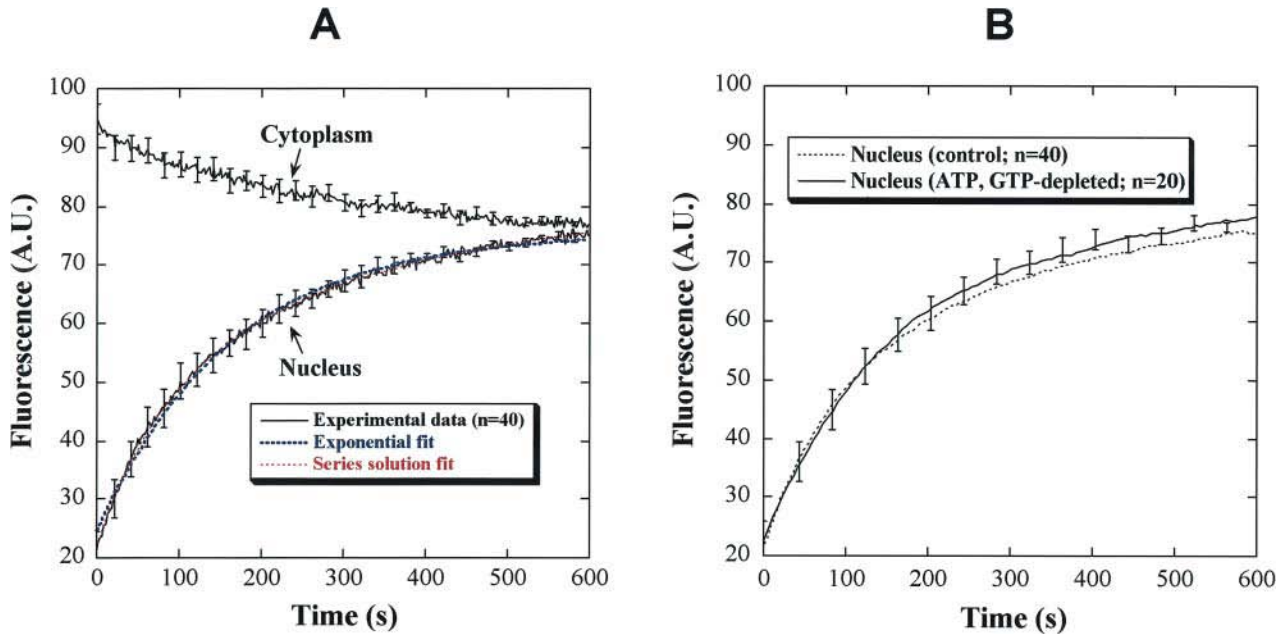

FIGURE 2 (*A*) Kinetics of nuclear fluorescence recovery after nuclear photobleaching. FRAP data were normalized to the pre-bleach values, which were arbitrarily set to 100. The time course of recovery (*solid black line*; mean ± SE; $n = 40$ from five independent experiments) was fit to the equation: $I = A^*(1-\exp(-t/\tau)) + I_0$ (*red dotted line*), where I = nuclear fluorescence intensity, A is a scaling constant, and I_0 is the nuclear fluorescence at the start of recovery (I_0). The parameters obtained from the fit were $A = 51.0$, $\tau = 164$ s, and $I_0 = 24.6$. The fluorescence decreased in the cytoplasm as EGFP diffused from the cytoplasm into the nucleus. For comparison, the time course of nuclear recovery was also fit to a series solution: $F(t) = F(\infty)\sum_{n=0}^{\infty}(-\beta)^n/n!(1 + n(1 + 2t/\tau_D))$ (*blue dotted line*), where β is the bleach depth parameter, and τ_D is the diffusive recovery time. τ_D obtained from the series solution fit was 135 s. (*B*) The kinetics of nuclear fluorescence recovery was independent of ATP/GTP depletion (mean ± SE, $n = 20$), implying passive diffusion of EGFP. ATP and GTP were depleted by a 30-min incubation of the cells in 6 mM DOG/1 μM FCCP at 37°C (curves smoothed for clarity).

much larger volume of the cytoplasm. For comparison with previous FRAP work on the diffusion of fluorescent molecules in the cells, we also fit the recovery of the nuclear EGFP signal with conventional FRAP formula, a series solution to an equation that describes recovery by free-diffusion in a two-dimensional plane (Axelrod et al., 1976). The time constant (τ) of recovery of nuclear fluorescence from this fit was 135 $\pm$ 1.4 s (mean $\pm$ SE, $n = 40$).

EGFP traffic through the NPC is presumably a passive diffusion process because EGFP is a 27-kDa ''barrel protein'' without an NLS (Ormo et al., 1996; Yang et al., 1996). To test whether there was an active component to EGFP movement across the NE, cellular ATP and GTP were depleted and the extent and kinetics of nuclear fluorescence recovery of EGFP in COS7 cells were measured. Intracellular ATP/GTP stores were depleted by applying 6 mM DOG (an inhibitor of glycolysis) and 1 μM FCCP (an oxidative phosphorylation inhibitor of mitochondria) for 30 min at 37°C (Breeuwer and Goldfarb, 1990; Kuznetsov et al., 1996; Lieberthal et al., 1998; Perez-Terzic et al., 1999; Raman and Atkinson, 1999). FRAP analysis revealed that ATP/GTP-depletion did not measurably affect the extent and kinetics of EGFP fluorescence recovery after nuclear photobleaching at 37°C as well as at 22°C (Fig. 2 *B*). We concluded that passive diffusion was the mechanism of EGFP traffic across the NPC.

EGFP diffusion was not blocked by perinuclear Ca^{2+} depletion

Depletion of perinuclear Ca^{2+} stores was shown to block passive diffusion of 10 kDa dextrans across the NPC (Greber and Gerace, 1995; Stehno-Bittel et al., 1995) in isolated nuclei, perhaps by the translocation of a transporter plug that occludes most of the central channel (Perez-Terzic et al., 1996). We tested this hypothesis in intact cells using the protein marker, EGFP. The perinuclear Ca^{2+} store was depleted and depletion was confirmed by a perinuclear-targeted YC (Fig. 3 *A*). Cameleon is a CFP and YFP linked by calmodulin and the calmodulin-binding peptide M13 (Miyawaki et al., 1997). When perinuclear [Ca^{2+}] is in the range of 60–400 μM (Miyawaki et al., 1997), binding of Ca^{2+} induces a conformational change in which calmodulin wraps around the M13 domain, drawing CFP and YFP together. YFP is then excited by FRET from the CFP. The targeting of the Ca^{2+}-sensitive indicator YC was achieved by fusing it with the first transmembrane domain of the LBR (Ellenberg et al., 1997). The LBR-YC is located in the perinuclear space and close to the inner nuclear membrane. When the perinuclear [Ca^{2+}] store was depleted by ionomycin, thapsigargin, BAPTA-AM, A23187, or TPEN, the FRET fluorescence ratio (YFP/CFP) declined by 10–20% (Fig. 3 *A*). Miyawaki et al. (1997) observed a similar 10–20% decline when mitochondria Ca^{2+} was buffered from 60–100 μM to <0.5 μM. This change corresponds to Ca^{2+} store emptying as defined functionally with the use of Ca^{2+} buffers and thapsigargin. In intact COS7 cells, the bidirectional EGFP traffic across the NE studied by photobleaching was not significantly changed after the perinuclear Ca^{2+} store was depleted (Fig. 3, *B* and *C*). Furthermore, the kinetics of nuclear FRAP in Ca^{2+}-depleted cells was not measurably different from control cells either at 37°C or at 22°C (Fig. 4).

Perez-Terzic et al. (1999) found that Ca^{2+} depletion of intact dextran/dye-microinjected rat cardiomyocytes blocked passive diffusion via the NPC. To rule out the possibility that NPC permeation block might be dependent on the cell type, we repeated these experiments in primary neonatal rat cardiomyocytes. Diffusion of EGFP across the NE was not blocked by perinuclear Ca^{2+} depletion with various agents (ionomycin, thapsigargin, BAPTA-AM, A23187, or TPEN) in rat primary cardiomyocytes (Fig. 5). Furthermore, similar FRAP was observed in HEK 293 cells and HM-1 (muscarinic type 1 receptor stably transfected) HEK cells (data not shown). FRAP was also similar in cells virally infected with EGFP (not shown).

To examine whether microinjection of dyes yielded different results from our FRAP experiments, we injected cells 5–15 min before confocal imaging. Ca^{2+} depletion of intact 10 kDa fluorescein-dextran-microinjected HM-1 HEK cells did not block its passive diffusion into the nucleus, whereas 70 kDa rhodamine-dextran was excluded from the nucleus (Fig. 6 *A*). Similar results were obtained in MDCK cells (Fig. 6 *B*) and in primary neonatal rat cardiomyocytes (data not shown).

EGFP diffusion between nucleus and cytoplasm was independent of the cell cycle

Many macromolecule distributions between the nucleus and cytoplasm vary with the stage of the cell cycle (White and Stelzer, 1999). In higher eukaryotes, the NE and NPC are dynamic, breaking down during late prophase and reassembling during late anaphase, telophase, and early G1 (Earnshaw and Pluta, 1994; Ellenberg et al., 1997; Foisner and Gerace, 1993; Wente, 2000; Zhang and Clarke, 2000). Particular interesting points are the onset and the end of mitosis, respectively, because the NPCs disassemble during prophase and metaphase, and reassemble during anaphase. We tested whether there was a difference in transnuclear passive diffusion during the cell cycle. COS7 cells were synchronized by 20-h treatment of aphidicolin. Aphidicolin inhibits S-phase entry by blocking α-DNA polymerase initiation of DNA synthesis (Reichard and Ehrenberg, 1983). Previous studies have shown that the G2/M boundary is reached $\sim$10 h after release from aphidicolin arrest (Krek and DeCaprio, 1995; Liao et al., 1997). Cells were washed after aphidicolin treatment and released from the G1/S boundary. Cell growth resumed and was confirmed by cell counting. The EGFP permeation experiments were carried out continuously for 24 h. A total of 96 cells were sampled

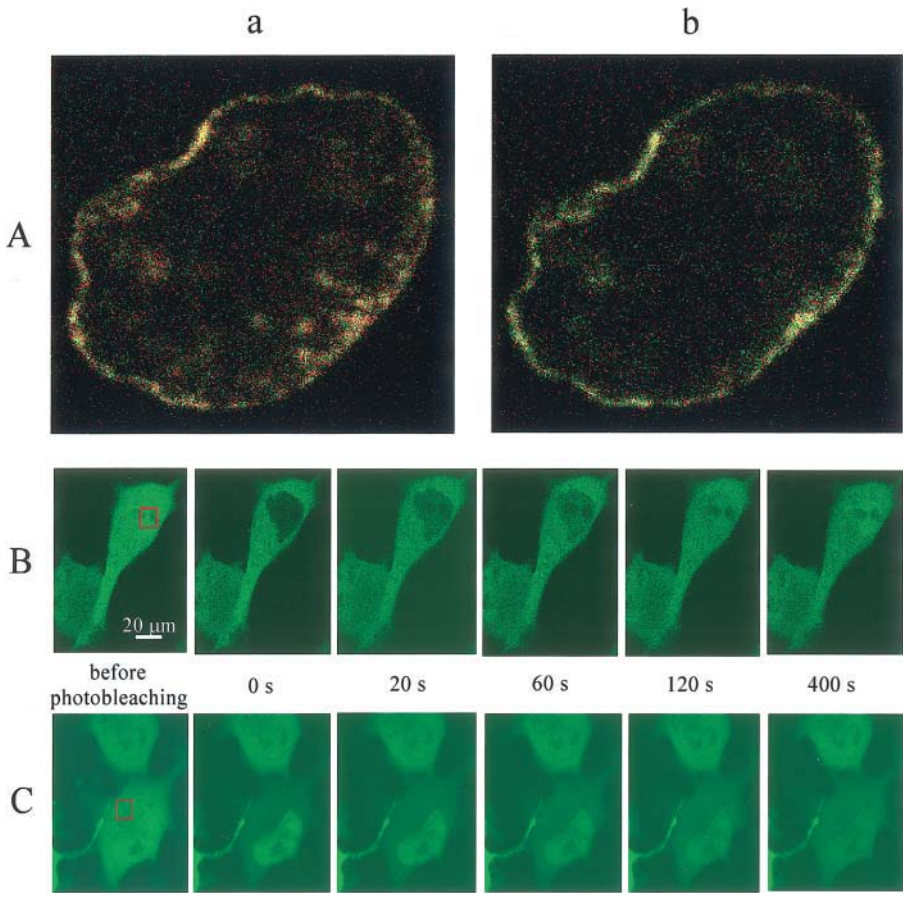

FIGURE 3 Nuclear transport of EGFP was not blocked by perinuclear Ca^{2+} depletion. (*A*) Perinuclear calcium depletion monitored by the perinuclear-targeted LBR-yellow cameleon (Miyawaki et al., 1997). 820-nm wavelength two-photon excitation of CFP resulted in YFP reemission at 535 nm. RGB-color overlay (*a*; yellow-red; 480-nm emission = green; 535-nm emission = red). When perinuclear $[Ca^{2+}]$ was depleted by 1 μM ionomycin in a low $[Ca^{2+}]$ buffer (estimated free $[Ca^{2+}] = 10$ nM), FRET declined by 19.1% (YFP/CFP fluorescence ratio; *b*; green). A similar decline in FRET was obtained when perinuclear $[Ca^{2+}]$ was depleted by 1–20 μM ionomycin for 20 min (19.6 ± 0.8%, mean ± SE), 3 μM thapsigargin for 90 min (17.4 ± 0.7%), 10–20 μM BAPTA-AM for 30 min (15.7 ± 0.6%), 50 μM A23187 for 20 min (18.4 ± 0.7%), or 100 μM TPEN for 60 min (17.5 ± 0.6%; 37°C; $n = 10$ from three independent experiments for each condition). This corresponds to complete Ca^{2+} store emptying as defined functionally with the use of Ca^{2+} buffers and thapsigargin. Our in situ calibration of the cameleon showed a similar dynamic range (YFP/CFP fluorescence ratio) as reported in Miyawaki et al. (1997). (*B*) Nuclear fluorescence recovery after nuclear photobleaching in a COS7 cell after perinuclear $[Ca^{2+}]$ depletion. Cells were treated in a low $[Ca^{2+}]$ buffer with 1 μM ionomycin for 20 min at 37°C before photobleaching. (*C*) Cytoplasmic fluorescence recovery after cytoplasmic photobleaching in a COS7 cell with perinuclear Ca^{2+} depletion. Cells were treated with 3 μM thapsigargin for 90 min at 37°C in a low $[Ca^{2+}]$ buffer before photobleaching. Fluorescence in the nucleus declined as fluorescent molecules diffused into the cytoplasm.

and EGFP permeation experiment was performed on individual cells for 10 min. EGFP diffusion was not blocked in any of the 96 cells measured at 15-min intervals (10 min of measurement followed by a 5-min delay to change the cell being studied) over 2.4 cell cycles (24 h; Fig. 7 *A*). In addition, the recovery of nuclear EGFP fluorescence in cells in anaphase or newly formed daughter cells was not significantly different from that of cells at other stages of the cell cycle (Fig. 7 *B*). The nuclear EGFP recovery of cells in the mitotic phase was complete within ~2 s, consistent with the absence of the NE, which presumably restricts the transnuclear diffusion and prevents fast equilibration. Finally, in pooled data from several experiments, none of 400 asynchronously growing cells exhibited any evidence of significant block. Thus EGFP diffusion was not measurably blocked during the cell cycle.

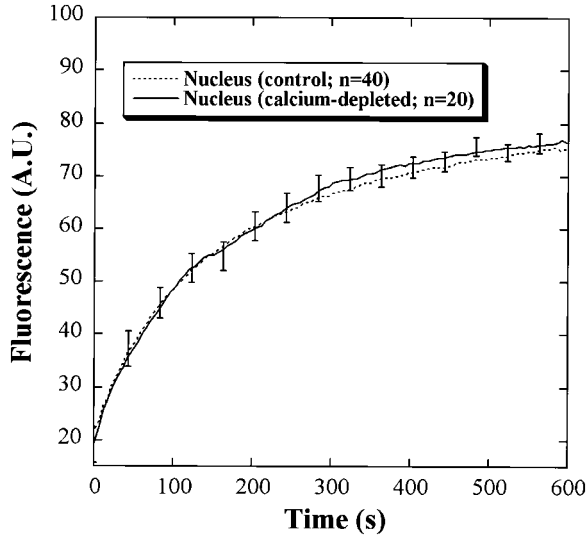

FIGURE 4 Nuclear fluorescence recovery after photobleaching of the nucleus in COS7 cells plotted as a function of time. FRAP in control (*dotted line*) and Ca^{2+}-depleted cells (*solid line*; mean ± SE, $n = 20$) were not measurably different. A.U. denotes arbitrary units of fluorescence intensity.

DISCUSSION

The major motivation for this work was to determine whether the changes observed in NPC permeation in isolated

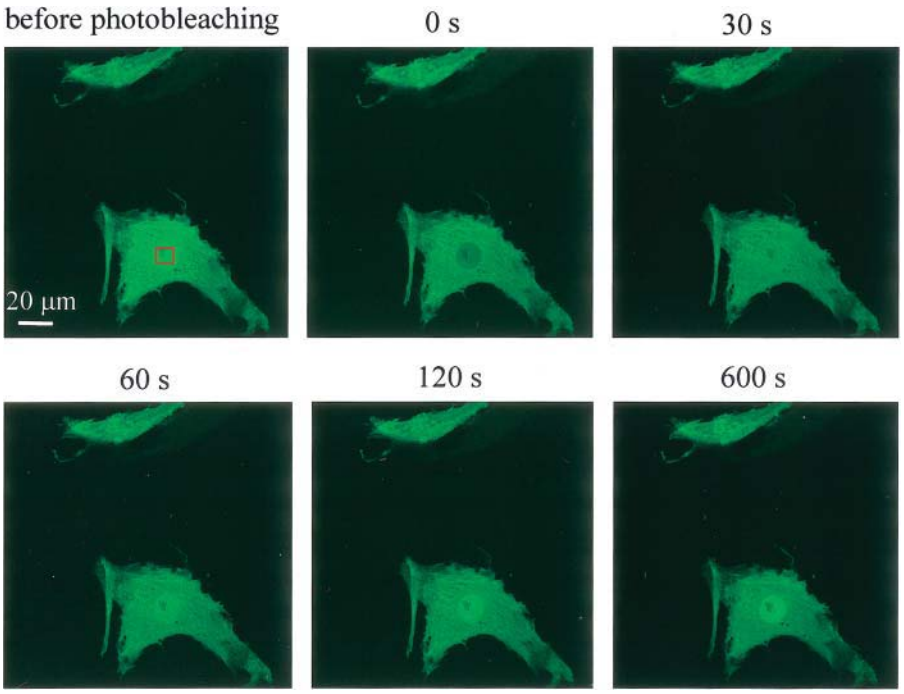

FIGURE 5 Diffusion of EGFP after nuclear photobleaching was not blocked by perinuclear Ca^{2+} depletion in rat primary cardiomyocytes. Rat primary cardiomyocytes were transfected with EGFP for 48 h. Before FRAP experiments, cardiomyocytes were selected by shape and by their ability to contract. Cells were treated with 3 μM thapsigargin for 90 min at 37°C in a low [Ca^{2+}] buffer before the diffusion assay was carried out. FRAP was not affected by perinuclear Ca^{2+} stores. Similar results were obtained when perinuclear [Ca^{2+}] was depleted by 1–20 μM ionomycin for 20 min, 3 μM thapsigargin for 90 min, 10–20 μM BAPTA-AM for 30 min, 50 μM A23187 for 20 min, or 100 μM TPEN for 60 min (37°C; $n =$ 24 for each condition).

nuclear preparations is pertinent to intact cells in vivo. The issue is important because agonists of G-protein-coupled receptors, most commonly Gq-linked receptors, deplete endoplasmic reticular Ca^{2+} significantly (histamine or ATP receptor activation depleted calcium in the ER from 60–400 μM to 1–50 μM in HeLa cells; Miyawaki et al., 1997). If such a Ca^{2+} release mechanism is able to alter diffusion into and out of the nucleus, it should have a major impact on the function of the cell. Dozens of proteins are known to transverse the NPC, often affecting transcription events that regulate the repertoire of proteins available throughout the cell (Kohler et al., 1999).

We examined the nuclear pore permeability of the heterologously expressed EGFP protein by irreversibly photobleaching the protein within defined cytoplasmic or nuclear volume and then measuring the rate of recovery by diffusion of unbleached EGFP into the compartment. We found that in intact cells, EGFP diffused bidirectionally across the NPC and was not altered either by depletion of perinuclear Ca^{2+} stores or by changes in the cell cycle at 37°C as well as at room temperature. This contrasts with studies of intact cardiomyocytes using microinjected dyes (Perez-Terzic et al., 1999).

Previously, depletion of perinuclear Ca^{2+} stores was shown to block both passive diffusion and active transport of intermediate-sized macromolecules across the NPC (Greber and Gerace, 1995). Entry of microinjected dextrans (10 kDa) into the nuclei of single mammalian cells was blocked upon depletion of perinuclear Ca^{2+} stores (Perez-Terzic et al., 1999). Entry of 10-kDa dextrans into isolated *Xenopus* oocyte nuclei was also blocked upon depletion of perinuclear Ca^{2+} stores (Stehno-Bittel et al., 1995). We show here that passive diffusion of EGFP across the NPC was not blocked by depletion of perinuclear Ca^{2+} stores in single intact mammalian cells using the noninvasive FRAP method. We have used a variety of agents to deplete perinuclear Ca^{2+} stores and confirmed the depletion of perinuclear Ca^{2+} stores using a nuclear cisterna-targeted Ca^{2+} indicator, yellow cameleon (see Results). It seems unlikely that our negative results were due to incomplete depletion of perinuclear Ca^{2+} stores, or due to differences in cell type. Lipofectamine, used to transfect cells, does not appear to affect nuclear transport because the kinetics and extent of EGFP permeation 8 h after transfection was not significantly different from that of cells examined three to five days after transfection. Furthermore, similar time courses of FRAP were observed in a stably transfected cell line and in cells transfected by viral infection.

Protein, mRNA, and ions traverse the nuclear membrane via the NPC under physiological conditions. EGFP, a stable and nontoxic 27-kDa fluorescent protein, is an ideal marker to study passive diffusion across the nuclear membrane inasmuch as the cell remains intact and microinjection is avoided. Microinjection used in previous studies can disrupt the cytoskeleton and alter cell volume regulation (Swaminathan et al., 1997). However, both our microinjection and FRAP experiments gave identical results in intact HM-1, MDCK, and rat primary cardiomyocytes.

The fluorescence intensity of EGFP within the nucleus (or cytoplasm) reached equilibrium within ~2 s indicating that EGFP diffuses freely within each cell compartment (Patterson et al., 1997; Seksek et al., 1997; Swaminathan et al., 1997; Tsien, 1998; Wachsmuth et al., 2000; Yokoe

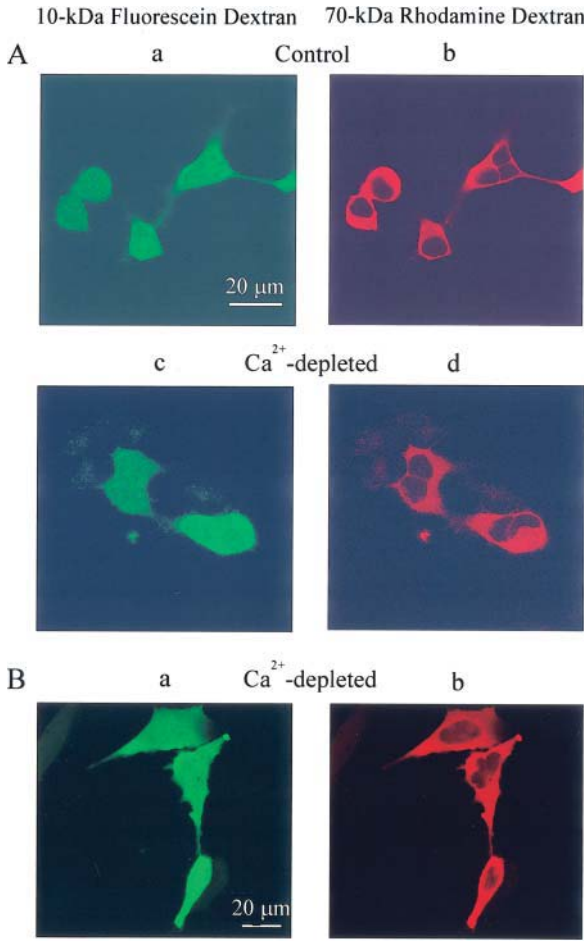

FIGURE 6 Ca^{2+} depletion of intact dextran/dye-microinjected HM-1 and MDCK cells did not block passive diffusion of 10kDa dextran. Each cell was microinjected with both 2.5 mg/ml 10 kDa fluorescein-dextran and 70 kDa rhodamine-dextran in injection buffer. (*A*) Confocal images of HM-1 cells after microinjection of 10 kDa fluorescein-dextran and 70 kDa rhodamine-dextran. In control cells (in normal Ca^{2+} medium), 10 kDa fluorescein-dextran diffused into the nucleus (*a*) whereas 70 kDa rhodamine-dextran was excluded from the nucleus (*b*). In cells preincubated at 37°C for 30 min in Ca^{2+}-free medium and 1.5 μM ionomycin, diffusion of 10 kDa fluorescein-dextran into the nucleus was not blocked (*c*) whereas 70 kDa rhodamine-dextran was excluded from the nucleus (*d*). (*B*) Confocal images of MDCK cells after microinjection of 10 kDa fluorescein-dextran and 70 kDa rhodamine-dextran. In MDCK cells preincubated at 37°C for 30 min in Ca^{2+}-free medium and 1.5 μM thapsigargin, diffusion of 10 kDa fluorescein-dextran into the nucleus was not blocked (*a*) whereas 70 kDa rhodamine-dextran was excluded from the nucleus (*b*). Similar results were obtained when perinuclear [Ca^{2+}] was depleted by ionomycin and BAPTA-AM (not shown).

and Meyer, 1996). However, fluorescence recovery of the nucleus required ~600 s to reach steady state, indicating that passive diffusion between the cytoplasm and the nucleus was significantly restricted by the reduced cross-sectional area through the NPCs. As a first approximation, we assume that diffusion through the sphere of the NE scales by cross-sectional area. Thus a 100-fold prolongation of diffusion should represent an ~100-fold lower cross-sectional area available for diffusion through the NPCs in comparison to diffusion in the absence of a membrane. The density of NPCs in the nuclear membrane (~10–20 pores/μm^2; Gerace and Burke, 1988) and the NPC pore diameter of ~40 nm (Feldherr et al., 1984; Ribbeck and Gorlich, 2001), yield an accessible cross-sectional area for diffusion through the NPCs in the range of ~1/80–1/40 of the total membrane area, consistent with the observed ~100-fold prolongation of fluorescence recovery of the nucleus. Furthermore, the ''effective'' nuclear pore diameter might well be significantly less than the numbers reported (Feldherr and Akin, 1990) and thus the slow recovery of a bleached nucleus is due to the limited number of nuclear pores.

Our study also examined the possibility that passive NPC diffusion by intermediate-sized molecules varies during the cell cycle. We found no marked change in NE permeation by EGFP during the cell cycle, including the onset of mitosis (G2/M boundary) and the end of mitosis. Feldherr and Akin detected difference at the end of mitosis by microinjecting colloidal gold (Feldherr and Akin, 1990). However, Swonson and McNeil studied the nuclear incorporation of fluorescein-labeled dextrans during division in fibroblasts and did not detect a difference in diffusion (Swanson and McNeil, 1987). Colloidal gold was concentrated in nuclei, presumably as a result of binding. Therefore it is difficult to compare Feldherr's results with ours using EGFP, a soluble molecule. In our experiments, none of 400 asynchronously growing cells exhibited any evidence of significant block. We cannot exclude less dramatic changes in diffusion due to regulation of the number of the NPCs in the NE as a function of cell cycle. Neither can we exclude the possibility that block occurred during short intervals (<5 min) between sampling times in the 24-h period studied.

In summary, we found by FRAP studies of intact COS7, HEK 293, and cardiac myocyte cells that the 27-kDa soluble EGFP protein diffused bidirectionally via NPC pores across the nuclear envelope. Although diffusion is slowed ~100-fold at the NE boundary compared to diffusion within the nucleo- or cytoplasm, this delay is in the expected range for the reduced cross-sectional area of the NPCs. In support of previous studies, the NPC is permeant to unregulated molecules up to ~60 kDa in size. We found no evidence for significant nuclear pore gating and block of EGFP diffusion by depletion of perinuclear Ca^{2+} stores, as assayed by a perinuclear-targeted Ca^{2+} indicator. We also found that EGFP exchange was not altered significantly during the cell cycle. These studies suggest that NPCs are largely open and allow intermediate-sized molecules that do not specifically bind to NPC transporters to freely cross the nuclear envelope.

We thank Drs. P. Ongusaha, E. Oancea, J. Chong, L. Runnels, M. Moran, S. Gapon, and Q. Shi for comments and assistance. We thank Drs. R.Y. Tsien and M. Badminton for LBR-YC, Dr. P. Ongusaha for Ad-EGFP, Dr. Bert Vogelstein for pADTrack-CMV (kan) and pAdEasy-1 (Amp), and Dr. A. Persechini for pcDIC35 and pcDIC49.

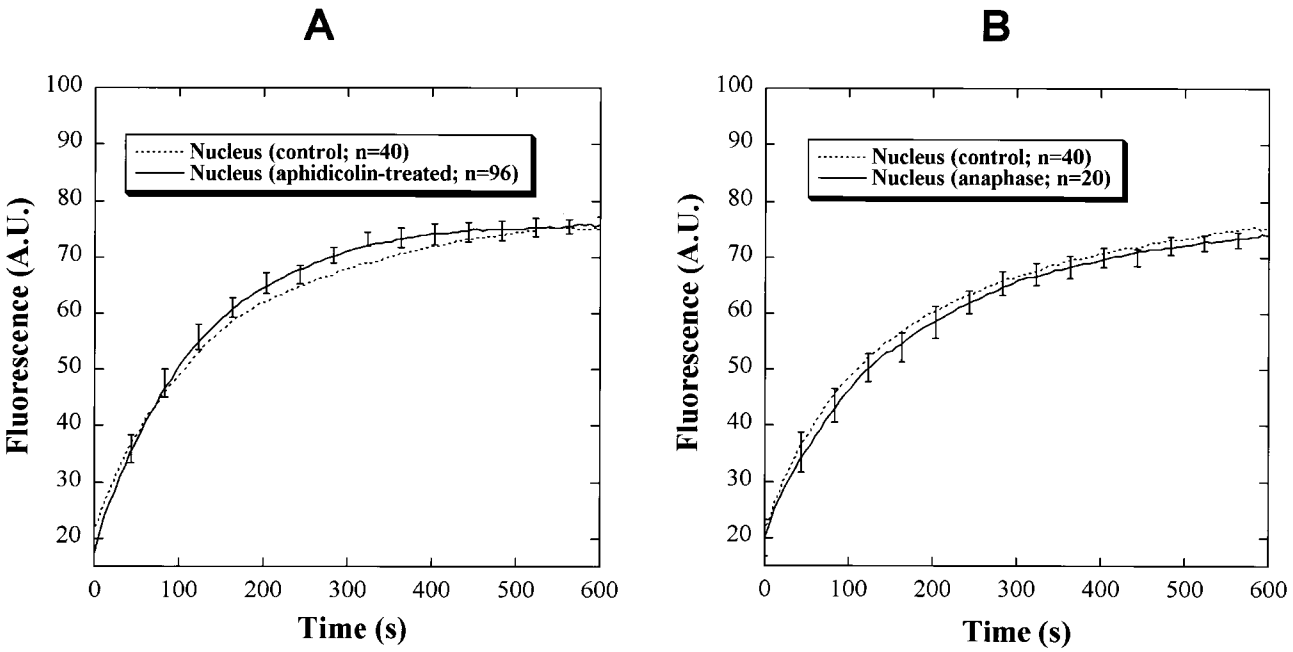

FIGURE 7 FRAP of the nucleus was not altered significantly during the cell cycle. (*A*) COS7 cells were synchronized with 20-h pretreatment of 15 μM aphidicolin (G1/S block; *solid line*) and compared to control cells (*dotted line*). FRAP assays were performed at 15-min intervals for a 24-h period. The transnuclear diffusion of EGFP was not blocked in any of the 96 cells observed (mean $\pm$ SE, $n = 96$). (*B*) FRAP assays were performed in cells at the end of mitosis (anaphase). The transnuclear diffusion of EGFP was not blocked in any of the 20 cells observed. The recovery of nuclear EGFP fluorescence in cells in anaphase (mean $\pm$ SE, $n = 20$) was not significantly different from that of cells at other stages of the cell cycle. Similar results were obtained from newly formed daughter cells.

This work was supported by the Howard Hughes Medical Institute and by the Department of Cardiology at Children's Hospital, Boston.

REFERENCES

Allen, T. D., J. M. Cronshaw, S. Bagley, E. Kiseleva, and M. W. Goldberg. 2000. The nuclear pore complex: mediator of translocation between nucleus and cytoplasm. *J. Cell Sci.* 113:1651–1659.

Axelrod, D., D. E. Koppel, J. Schlessinger, E. Elson, and W. W. Webb. 1976. Mobility measurement by analysis of fluorescence photobleaching recovery kinetics. *Biophys. J.* 16:1055–1069.

Breeuwer, M., and D. S. Goldfarb. 1990. Facilitated nuclear transport of histone H1 and other small nucleophilic proteins. *Cell.* 60:999–1008.

Danker, T., and H. Oberleithner. 2000. Nuclear pore function viewed with atomic force microscopy. *Pflugers Arch.* 439:671–681.

Earnshaw, W. C., and A. F. Pluta. 1994. Mitosis. *Bioessays.* 16:639–643.

Ellenberg, J., E. D. Siggia, J. E. Moreira, C. L. Smith, J. F. Presley, H. J. Worman, and J. Lippincott-Schwartz. 1997. Nuclear membrane dynamics and reassembly in living cells: targeting of an inner nuclear membrane protein in interphase and mitosis. *J. Cell Biol.* 138:1193–1206.

Fatatis, A., and R. J. Miller. 1999. Cell cycle control of PDGF-induced Ca^{2+} signaling through modulation of sphingolipid metabolism. *FASEB J.* 13:1291–1301.

Feldherr, C. M., and D. Akin. 1990. The permeability of the nuclear envelope in dividing and nondividing cell cultures. *J. Cell Biol.* 111:1–8.

Feldherr, C. M., E. Kallenbach, and N. Schultz. 1984. Movement of a karyophilic protein through the nuclear pores of oocytes. *J. Cell Biol.* 99:2216–2222.

Foisner, R., and L. Gerace. 1993. Integral membrane proteins of the nuclear envelope interact with lamins and chromosomes, and binding is modulated by mitotic phosphorylation. *Cell.* 73:1267–1279.

Gerace, L., and B. Burke. 1988. Functional organization of the nuclear envelope. *Annu. Rev. Cell Biol.* 4:335–374.

Greber, U. F., and L. Gerace. 1995. Depletion of calcium from the lumen of endoplasmic reticulum reversibly inhibits passive diffusion and signal-mediated transport into the nucleus. *J. Cell Biol.* 128:5–14.

He, T. C., S. Zhou, L. T. da Costa, J. Yu, K. W. Kinzler, and B. Vogelstein. 1998. A simplified system for generating recombinant adenoviruses. *Proc. Natl. Acad. Sci. USA.* 95:2509–2514.

Hicks, G. R., and N. V. Raikhel. 1995. Protein import into the nucleus: an integrated view. *Annu. Rev. Cell Dev. Biol.* 11:155–188.

Keminer, O., and R. Peters. 1999. Permeability of single nuclear pores. *Biophys. J.* 77:217–228.

Kohler, M., H. Haller, and E. Hartmann. 1999. Nuclear protein transport pathways. *Exp. Nephrol.* 7:290–294.

Krek, W., and J. A. DeCaprio. 1995. Cell synchronization. *Methods Enzymol.* 254:114–124.

Kuznetsov, G., K. T. Bush, P. L. Zhang, and S. K. Nigam. 1996. Perturbations in maturation of secretory proteins and their association with endoplasmic reticulum chaperones in a cell culture model for epithelial ischemia. *Proc. Natl. Acad. Sci. USA.* 93:8584–8589.

Liao, J., N. O. Ku, and M. B. Omary. 1997. Stress, apoptosis, and mitosis induce phosphorylation of human keratin 8 at Ser-73 in tissues and cultured cells. *J. Biol. Chem.* 272:17565–17573.

Lieberthal, W., S. A. Menza, and J. S. Levine. 1998. Graded ATP depletion can cause necrosis or apoptosis of cultured mouse proximal tubular cells. *Am. J. Physiol.* 274:F315–F327.

Liu, Y., D. K. Cheng, G. J. Sonek, M. W. Berns, C. F. Chapman, and B. J. Tromberg. 1995. Evidence for localized cell heating induced by infrared optical tweezers. *Biophys. J.* 68:2137–2144.

Majewska, A., E. Brown, J. Ross, and R. Yuste. 2000. Mechanisms of calcium decay kinetics in hippocampal spines: role of spine calcium pumps and calcium diffusion through the spine neck in biochemical compartmentalization. *J. Neurosci.* 20:1722–1734.

Miyawaki, A., J. Llopis, R. Heim, J. M. McCaffery, J. A. Adams, M. Ikura, and R. Y. Tsien. 1997. Fluorescent indicators for Ca^{2+} based on green fluorescent proteins and calmodulin. *Nature.* 388:882–887.

Ormo, M., A. B. Cubitt, K. Kallio, L. A. Gross, R. Y. Tsien, and S. J. Remington. 1996. Crystal structure of the Aequorea victoria green fluorescent protein. *Science.* 273:1392–1395.

Patterson, G. H., S. M. Knobel, W. D. Sharif, S. R. Kain, and D. W. Piston. 1997. Use of the green fluorescent protein and its mutants in quantitative fluorescence microscopy. *Biophys. J.* 73:2782–2790.

Perez-Terzic, C., A. M. Gacy, R. Bortolon, P. P. Dzeja, M. Puceat, M. Jaconi, F. G. Prendergast, and A. Terzic. 1999. Structural plasticity of the cardiac nuclear pore complex in response to regulators of nuclear import. *Circ. Res.* 84:1292–1301.

Perez-Terzic, C., J. Pyle, M. Jaconi, L. Stehno-Bittel, and D. E. Clapham. 1996. Conformational states of the nuclear pore complex induced by depletion of nuclear Ca^{2+} stores. *Science.* 273:1875–1877.

Raman, N., and S. J. Atkinson. 1999. Rho controls actin cytoskeletal assembly in renal epithelial cells during ATP depletion and recovery. *Am. J. Physiol.* 276:C1312–C1324.

Reichard, P., and A. Ehrenberg. 1983. Ribonucleotide reductase—a radical enzyme. *Science.* 221:514–519.

Ribbeck, K., and D. Gorlich. 2001. Kinetic analysis of translocation through nuclear pore complexes. *EMBO J.* 20:1320–1330.

Romoser, V. A., P. M. Hinkle, and A. Persechini. 1997. Detection in living cells of Ca^{2+}-dependent changes in the fluorescence emission of an indicator composed of two green fluorescent protein variants linked by a calmodulin-binding sequence. A new class of fluorescent indicators. *J. Biol. Chem.* 272:13270–13274.

Rost, F. W. D. 1992. Fluorescence Microscopy. Cambridge University Press, Cambridge, UK.

Schindler, M., and L. W. Jiang. 1987. Fluorescence redistribution after photobleaching as a tool for dissecting the control elements of nucleocytoplasmic transport. *Methods Enzymol.* 141:447–459.

Seksek, O., J. Biwersi, and A. S. Verkman. 1997. Translational diffusion of macromolecule-sized solutes in cytoplasm and nucleus. *J. Cell Biol.* 138:131–142.

Shahin, V., T. Danker, K. Enss, R. Ossig, and H. Oberleithner. 2001. Evidence for Ca^{2+}- and ATP-sensitive peripheral channels in nuclear pore complexes. *FASEB J.* 15:1895–1901.

Stehno-Bittel, L., C. Perez-Terzic, and D. E. Clapham. 1995. Diffusion across the nuclear envelope inhibited by depletion of the nuclear Ca^{2+} store. *Science.* 270:1835–1838.

Stoffler, D., K. N. Goldie, B. Feja, and U. Aebi. 1999. Calcium-mediated structural changes of native nuclear pore complexes monitored by time-lapse atomic force microscopy. *J. Mol. Biol.* 287:741–752.

Strubing, C., and D. E. Clapham. 1999. Active nuclear import and export is independent of luminal Ca^{2+} stores in intact mammalian cells. *J. Gen. Physiol.* 113:239–248.

Svoboda, K., D. W. Tank, and W. Denk. 1996. Direct measurement of coupling between dendritic spines and shafts. *Science.* 272:716–719.

Swaminathan, R., C. P. Hoang, and A. S. Verkman. 1997. Photobleaching recovery and anisotropy decay of green fluorescent protein GFP-S65T in solution and cells: cytoplasmic viscosity probed by green fluorescent protein translational and rotational diffusion. *Biophys. J.* 72:1900–1907.

Swanson, J. A., and P. L. McNeil. 1987. Nuclear reassembly excludes large macromolecules. *Science.* 238:548–550.

Tsien, R. Y. 1998. The green fluorescent protein. *Annu. Rev. Biochem.* 67:509–544.

Tsien, R. Y., and A. Waggoner. 1995. Fluorophores for Confocal Microscopy. *In* Handbook of Biological Confocal Microscopy. J. Pawley, editor. Plenum, New York. 267–277.

Wachsmuth, M., W. Waldeck, and J. Langowski. 2000. Anomalous diffusion of fluorescent probes inside living cell nuclei investigated by spatially-resolved fluorescence correlation spectroscopy. *J. Mol. Biol.* 298:677–689.

Wang, H., and D. E. Clapham. 1999. Conformational changes of the in situ nuclear pore complex. *Biophys. J.* 77:241–247.

Wente, S. R. 2000. Gatekeepers of the nucleus. *Science.* 288:1374–1377.

White, J., and E. Stelzer. 1999. Photobleaching GFP reveals protein dynamics inside live cells. *Trends Cell Biol.* 9:61–65.

Yang, F., L. G. Moss, and G. N. Phillips, Jr. 1996. The molecular structure of green fluorescent protein. *Nat. Biotechnol.* 14:1246–1251.

Yokoe, H., and T. Meyer. 1996. Spatial dynamics of GFP-tagged proteins investigated by local fluorescence enhancement. *Nat. Biotechnol.* 14:1252–1256.

Zhang, C., and P. R. Clarke. 2000. Chromatin-independent nuclear envelope assembly induced by Ran GTPase in Xenopus egg extracts. *Science.* 288:1429–1432.